

Thermodynamic aspect: kinetics of the reduction of dicyanobis(phen)iron(III) by acetylferrocene and methylferrocenemethanol

Rozina Khattak^{1,2} · Misbah Nazir² · Shazia Summer³ · Murtaza Sayed⁴ · Aaliya Minhaz¹ · Iftikhar I. Naqvi²

Received: 19 July 2017 / Accepted: 31 October 2017 / Published online: 11 November 2017
© Institute of Chemistry, Slovak Academy of Sciences 2017

Abstract Protonation plays an important role in the redox reactions. We observed this leading role during the reduction of $[\text{Fe}^{\text{III}}(\text{phen})_2(\text{CN})_2]^+$ by FcCOMe and FcCHOHMe . The kinetic data showed that the reaction(s) followed a complex kinetics due to the formation of protonated acetylferrocene (FcC^+OHMe), and or, protonated α -methylferrocenemethanol ($\text{FcCHO}^+\text{H}_2\text{Me}$) in aqueous dioxane (80% v/v). Our results helped us to conclude that the reactions were completed in three phases. An overall zeroth order was observed in the first phase of the reactions. In the second phase, the kinetic data showed an overall second order reaction. The third phase was a complex phase where the rate of redox reactions and the insolubility of the neutral product ($[\text{Fe}^{\text{II}}(\text{phen})_2(\text{CN})_2]$) competed with each other. We studied the effect of different factors to identify the reacting entities, which take part in the rate-determining step of each reaction in the second phase. Consequently, we

determined the effects of selected factors upon the observed pseudo-first order rate constant(s) (k'_{obs}) of each reaction. The value of k'_{obs} increased upon addition of protons in the reaction mixture in case of FcCOMe , and it decreased during the oxidation of FcCHOHMe . Meanwhile, upon enhancing the ionic strength, we observed an increase in k'_{obs} for FcCOMe , and no change in the value of k'_{obs} during the reaction of FcCHOHMe . However, a decrease in k'_{obs} was noticed upon increasing the dielectric constant of the reaction mixture when the reductant was FcCOMe , and no effect was observed in case of FcCHOHMe . Together, these results suggested oxidation of FcC^+OHMe and FcCHOHMe in the slow-step, and FcCOMe and $\text{FcCHO}^+\text{H}_2\text{Me}$ during the fast-step. We refined our results by estimating the thermodynamic parameters of activation. The low values of activation energy and enthalpy of activation confirmed that the reduction of $[\text{Fe}^{\text{III}}(\text{phen})_2(\text{CN})_2]^+$ hardly depends upon temperature when the reducing agent is FcCOMe . The outcomes justified that the rate of reaction depends upon the unsaturated FcC^+OHMe . This intermediate species contain a 'carbonium ion', which is very reactive and energetic. We obtained comparatively high values of the activation energy and enthalpy of activation for the reaction between $[\text{Fe}^{\text{III}}(\text{phen})_2(\text{CN})_2]^+$ and FcCHOHMe . The results show that FcCHOHMe is a saturated and stable compound that leads the slow-step and controls the rate of reaction.

This article belongs to the "Coordination and Bioinorganic Conference".

Electronic supplementary material The online version of this article (<https://doi.org/10.1007/s11696-017-0334-1>) contains supplementary material, which is available to authorized users.

✉ Rozina Khattak
rznkhattak@yahoo.com; rznkhattak@sbbwu.edu.pk

- 1 Department of Chemistry, Shaheed Benazir Bhutto Women University, Peshawar, Pakistan
- 2 Department of Chemistry, University of Karachi, Karachi 75270, Pakistan
- 3 Department of Chemistry, Jinnah University for Women, V-C Nazimabad, Karachi, Pakistan
- 4 National Center of Excellence in Physical Chemistry, University of Peshawar, Peshawar 25120, Pakistan

Keywords Acetylferrocene · α -Methylferrocenemethanol · Dicyanobis(phen)iron(III) · Outer-sphere mechanism

Introduction

Redox reaction(s) proceeds through the donation of electron(s) and its acceptance between the participant reactants. Either of the two, i.e., electron releasing (oxidation) or electron withdrawing (reduction) capacity of a reactant, depends upon the condition(s) in which the specific reaction takes place (Khattak et al. 2008; Khattak 2011; Khattak et al. 2016; Summer et al. 2016). There are several such factors that affect the reduction–oxidation tendency of the chemical species and alter the reaction mechanism consequently than the one, which we expect (Khattak et al. 2008). The capability of electron withdrawing nature of any chemical entity is termed as, “reduction potential” and denoted by $E_{1/2}$. Out of a number of factors, the reduction potential of any chemical species may vary with the nature of a solvent and the electrolyte itself or a supporting electrolyte present in the vicinity (Connelly and Geiger 1996). The mechanistic paths in an electron exchange process may thus get altered by changing the solvent medium (water, organic solvent or their mixture). Through studying the chemical kinetics and evaluating activation parameters, it is possible to identify the major reaction pathway. Kinetic studies are therefore important to determine the rates of different reactions and to propose the rate law in the view of results regarding crucial reactions.

A few studies describe the reduction of dicyanobis(phen) iron(III) ($E_{1/2}$ 800 mV) by reducing agents of biological importance such as ascorbic acid, hydroquinone, catechol, sulfatoiron and rusticyanin (Pelizzetti et al. 1978; Blake et al. 1991; Takagi et al. 1995; Matsumoto et al. 1997). These studies propose an outer-sphere mechanism for all of these reactions and estimates activation parameters for some of them. The applications of ferrocene and its derivatives in medicine and agriculture drew our attention. Their effects as antifungal, antiparasitic, anticancer, antibacterial and use as biosensors have been reported in medicinal chemistry (Saleem et al. 2015; Patra and Gasser 2017; Realista et al. 2017). However, they have been specified as agrochemicals and chemosensors in agriculture (Floris 2015). The reduction potentials of acetylferrocene and a number of other derivatives of ferrocene in acetonitrile were determined by titrimetric analysis through oxidation with Cu(II) (Quirk and Kratochvil 1970). Studies on the kinetics of the redox reactions between some ferrocene derivatives have also been published, and an outer-sphere mechanism has been suggested (Pladziejewicz and Espenson 1973). Although the data are comprehensive, the study is inadequate with respect to acetylferrocene ($E_{1/2}$ 740 mV). The data pertaining to the reactions of acetylferrocene mainly emphasize upon the synthesis of its derivatives, its role as a catalyst in the electrocatalytic oxidation of *N*-acetyl-L-cysteine and sulfite at a glassy carbon electrode, and its electrochemical

characteristics (Sasaki and Pittman 1973; Baciocchi et al. 1993; Xu et al. 1994; Jong et al. 1999; Gao et al. 2005a, b; Casas et al. 2007). Meanwhile, a few reports highlight the importance and use of ferrocene-containing alcohols including α -methylferrocenemethanol ($E_{1/2}$ 204 mV) in chemotherapy (Osella et al. 2000; Shago et al. 2007).

There are limited reports which approach the detailed kinetic and mechanistic analyses of the redox reactions of FcCOMe and FcCHOHMe by other transition metals or their complexes. The spectrophotometric investigations are rare, however. We studied the kinetics and determined the thermodynamic aspect of the reduction of dicyanobis(phen) iron(III) by acetylferrocene and α -methylferrocenemethanol in the mixed solvent system (aqueous dioxane).

Experimental

We used analar grade materials; 1,4-dioxane (Merck), 1,10-phenanthroline monohydrate (Merck), nitric acid (65% extra pure, Merck), potassium nitrate (Merck), ferrous ammonium sulfate hexahydrate (BDH), potassium cyanide (Scharlau), acetylferrocene 95% (Acros Organics), and α -methylferrocenemethanol 95–97% (Acros Organics). We synthesized and purified the nitrate salt of dicyanobis(phen)iron(III) by applying the reported procedures (Schilt 1960; Khattak 2011).

The spectral characterization of the compounds was performed on a Shimadzu UV-160A UV/Vis spectrophotometer in UV/Vis region. The Carlo Erba 1106 elemental analyser was used to carry out elemental analysis. The IKA Combimag RCH assembly was used to heat and stir the solutions. Two pH meters of different companies were used to measure the pH of the solutions. One of them was Mettler Toledo MP-220 basic pH/mV/°C meter, and the other one was HANNA HI 8314 membrane pH meter equipped with SCHOTT pH-electrode BlueLine 25PH (pH 0–14/– 5 to + 80 °C/Gel). The temperature of the solutions was maintained by Haake KT 33 water bath.

A home-built rapid reaction monitoring system was used to acquire kinetic data. The instrumental assembly consisted of a Spectronic 21 (Milton Roy Company), Vernier LabPro[®], and a desktop computer. We used Logger Pro 3.2 software. We mixed the solutions manually in a 3 mL cuvette with the help of disposable syringes (10 mL). All solutions were mixed in the cuvette except reducing or oxidizing agent prior to starting the reaction(s). The setup was maintained in such a way that the syringe without needle was inserted into the cuvette through which the top of the cuvette was completely covered. After starting the data acquisition, the plunger was pushed to withdraw the remaining reactant (1–1.5 mL) into the cuvette at once, and to start the reaction. This produced a graph of absorbance versus time. We recorded the formation of $[\text{Fe}^{\text{II}}(\text{phen})_2(\text{CN})_2]$ at 530 nm.

The reactions were studied under the condition of pseudo-first order. The concentration of FcCOMe, and, or FcCHOHMe was always in excess over $[\text{Fe}^{\text{III}}(\text{phen})_2(\text{CN})_2]^+$. The kinetic data showed that the reduction of $[\text{Fe}^{\text{III}}(\text{phen})_2(\text{CN})_2]^+$ by FcCOMe and FcCHOHMe completed in three phases (Figures S1–S2, supplementary data). The first phase involved approximately 30 and 51 percent fraction of the reaction of FcCOMe and FcCHOHMe, respectively. The reaction(s) followed zeroth order with respect to $[\text{Fe}^{\text{III}}(\text{phen})_2(\text{CN})_2]^+$ and FcCOMe, and or, FcCHOHMe. The reaction(s) was/were overall second order in the second phase; first order with respect to each of the oxidizing and the reducing agent. The third phase was a complex phase, where two different processes competed with each other and affected the results in that phase. We recorded an increase in absorbance along time considering the large value of the molar absorptivity (ϵ , $\text{M}^{-1} \text{cm}^{-1}$) of $[\text{Fe}^{\text{II}}(\text{phen})_2(\text{CN})_2]$ as compared to its oxidized form $[\text{Fe}^{\text{III}}(\text{phen})_2(\text{CN})_2]^+$. This helped us to follow the reactions spectrophotometrically by using a low concentration range (0.05–0.15 mM) of $[\text{Fe}^{\text{III}}(\text{phen})_2(\text{CN})_2]^+$. Considering this range, the excess concentration of FcCOMe and FcCHOHMe to maintain pseudo-first order condition, was also in a range of 0.08–1.88 mM. Through these arrangements, we were able to study the reactions in 80% aqueous dioxane mixture without any interference such as precipitation of either of the organometallic compounds, FcCOMe or FcCHOHMe, and $[\text{Fe}^{\text{III}}(\text{phen})_2(\text{CN})_2]^+$ in aqueous dioxane medium. However, we observed precipitates of the neutral $[\text{Fe}^{\text{II}}(\text{phen})_2(\text{CN})_2]$ in the end of the reaction(s) as the concentration of the product ($[\text{Fe}^{\text{II}}(\text{phen})_2(\text{CN})_2]$) reached its maximum value with respect to time. After filtration and spectrophotometric analysis, we observed the similar spectrum of $[\text{Fe}^{\text{II}}(\text{phen})_2(\text{CN})_2]$ with consistent wavelength maximum to the reported one (Schilt 1960). The spectra confirmed the precipitates to be $[\text{Fe}^{\text{II}}(\text{phen})_2(\text{CN})_2]$, which is one of the products of each reaction. This decrease in the solubility of $[\text{Fe}^{\text{II}}(\text{phen})_2(\text{CN})_2]$ in aqueous dioxane made the measurements complicated at the end of the reactions because of the competition of the rate of redox reaction(s) with the rate of decrease in the solubility of $[\text{Fe}^{\text{II}}(\text{phen})_2(\text{CN})_2]$. Consequently, the absorbance was changed (decreased) along time and we did not observe the data that continue fitting the integrated rate law of first order in the third phase, correctly. A straight line was monitored in the second phase of the reaction that started bending in the third phase with again straight line character to the end of the reactions, but with a low value of the slope. This confirms our observations. We mentioned average values (average of 3–6) of the rate constants. This is noteworthy that we have determined the pseudo-first order rate constant ($k'_{\text{obs}}/\text{s}^{-1}$) by integration method. We also evaluated the zeroth order kinetic data by integrated rate equations, but, we have used the value of slope ($\epsilon b k_{\text{obs}}/\text{s}^{-1}$) instead of zero order rate constant ($k_{\text{obs}}/\text{M s}^{-1}$). The symbol ϵ represents

molar absorptivity (M cm^{-1}) of dicyanobis(phen)iron(II) and b denotes path length of the cuvette (1 cm). This reduces the slope to ($\epsilon k_{\text{obs}}/\text{s}^{-1}$), where molar absorptivity is a constant and it does not affect the zero order rate constant.

Following equations were used to evaluate the rate constants.

Under pseudo-first order condition:

$$[\text{Fe}^{\text{III}}(\text{phen})_2(\text{CN})_2]^+ \ll \text{FcCOMe or FcCHOHMe.}$$

As we know, for a zero order reaction or the first phase of the reaction,

$$\begin{aligned} \text{Rate} &= \frac{d[\text{Fe}^{\text{II}}(\text{phen})_2(\text{CN})_2]}{dt} \\ &= k_1 [\text{Fe}^{\text{III}}(\text{phen})_2(\text{CN})_2]^+ [\text{FcCOMe/FcCHOHMe}]^0, \end{aligned} \quad (1)$$

\therefore

$$[\text{Fe}^{\text{III}}(\text{phen})_2(\text{CN})_2]^+ \ll [\text{FcCOMe/FcCHOHMe}] \quad (2)$$

\therefore

$$k_1 [\text{FcCOMe/FcCHOHMe}]^0 = k_{\text{obs}},$$

$$\frac{d[\text{Fe}^{\text{II}}(\text{phen})_2(\text{CN})_2]}{dt} = k_{\text{obs}} [\text{Fe}^{\text{III}}(\text{phen})_2(\text{CN})_2]^+ \quad (3)$$

$$\frac{d[\text{Fe}^{\text{II}}(\text{phen})_2(\text{CN})_2]}{[\text{Fe}^{\text{III}}(\text{phen})_2(\text{CN})_2]^+} = k_{\text{obs}} dt, \quad (4)$$

\therefore

$$[\text{Fe}^{\text{III}}(\text{phen})_2(\text{CN})_2]^+ = 1 \quad (5)$$

$$\int_{[\text{Fe}^{\text{II}}(\text{phen})_2(\text{CN})_2]_0}^{[\text{Fe}^{\text{II}}(\text{phen})_2(\text{CN})_2]_t} d[\text{Fe}^{\text{II}}(\text{phen})_2(\text{CN})_2] = k_{\text{obs}} \int_0^t dt,$$

$$[\text{Fe}^{\text{II}}(\text{phen})_2(\text{CN})_2]_t - [\text{Fe}^{\text{II}}(\text{phen})_2(\text{CN})_2]_0 = k_{\text{obs}} t, \quad (6)$$

\therefore

$$\begin{aligned} [\text{Fe}^{\text{II}}(\text{phen})_2(\text{CN})_2]_0 &= 0 \quad (\text{initial concentration of the product}) \\ [\text{Fe}^{\text{II}}(\text{phen})_2(\text{CN})_2]_t &= k_{\text{obs}} t, \end{aligned} \quad (7)$$

where

$$k_{\text{obs}} = k_1 [\text{FcCOMe/FcCHOHMe}]^0, \quad (2)$$

$$\begin{aligned} \therefore \\ [\text{FcCOMe}/\text{FcCHOHMe}]^0 = 1 \\ \therefore \\ k_{\text{obs}} = k_1, \end{aligned} \quad (8)$$

According to Beer-Lambert law:

$$\text{Absorbance} = \varepsilon b c$$

If we consider our reactions and formation of the product ($[\text{Fe}^{\text{II}}(\text{phen})_2(\text{CN})_2]$) along time, then, we obtain following equation:

$$\frac{[\text{Absorbance}]_t}{\varepsilon b} = [\text{Fe}^{\text{II}}(\text{phen})_2(\text{CN})_2]_t, \quad (9)$$

$$\begin{aligned} \therefore \\ b = 1 \text{ cm} \\ \frac{[\text{Absorbance}]_t}{\varepsilon} = [\text{Fe}^{\text{II}}(\text{phen})_2(\text{CN})_2]_t \end{aligned} \quad (10)$$

After comparing and solving Eqs. (7, 8) and (10), we get Eq. (11) as follows:

$$\begin{aligned} \frac{[\text{Absorbance}]_t}{\varepsilon} = [\text{Fe}^{\text{II}}(\text{phen})_2(\text{CN})_2]_t = k_{\text{obs}} t = k_1 t \\ [\text{Absorbance}]_t = \varepsilon k_{\text{obs}} t = \varepsilon k_1 t \end{aligned} \quad (11)$$

We obtained straight line(s) when absorbance at time point 't' was plotted against time, according to Eq. (11). The line(s) pass(es) origin and yielded value(s) of the slope. The slope of the plot(s) was the product of molar absorptivity and zero order rate constant with a dimension (s^{-1}) similar to that of the pseudo-first order rate constant. However, in certain cases, small discrepancy from passing through the origin represented deviation or experimental error.

Meanwhile, for the first order reaction or the second phase of the reaction(s), we derived following resulting equation and interpreted our data accordingly:

$$\begin{aligned} \text{Rate} &= \frac{d[\text{Fe}^{\text{II}}(\text{phen})_2(\text{CN})_2]}{dt} \\ &= k_2 [\text{Fe}^{\text{III}}(\text{phen})_2(\text{CN})_2^+] [\text{FcCOMe}/\text{FcCHOHMe}], \end{aligned} \quad (12)$$

$$\begin{aligned} \therefore \\ [\text{Fe}^{\text{III}}(\text{phen})_2(\text{CN})_2^+] \ll [\text{FcCOMe}/\text{FcCHOHMe}] \\ \therefore \\ k_2 [\text{FcCOMe}/\text{FcCHOHMe}] = k'_{\text{obs}}, \end{aligned} \quad (13)$$

$$\frac{d[\text{Fe}^{\text{II}}(\text{phen})_2(\text{CN})_2]}{dt} = k'_{\text{obs}} [\text{Fe}^{\text{III}}(\text{phen})_2(\text{CN})_2^+] \quad (14)$$

As we know that the consumption of $[\text{Fe}^{\text{III}}(\text{phen})_2(\text{CN})_2^+]$ is equal to the formation of $[\text{Fe}^{\text{II}}(\text{phen})_2(\text{CN})_2]$; therefore, Eq. (14) is solved to Eq. (17) as follows:

$$[\text{Fe}^{\text{III}}(\text{phen})_2(\text{CN})_2^+] = [\text{Fe}^{\text{II}}(\text{phen})_2(\text{CN})_2]$$

$$\begin{aligned} \frac{d[\text{Fe}^{\text{II}}(\text{phen})_2(\text{CN})_2]}{[\text{Fe}^{\text{III}}(\text{phen})_2(\text{CN})_2^+]} &= k'_{\text{obs}} dt \\ \frac{d[\text{Fe}^{\text{II}}(\text{phen})_2(\text{CN})_2]}{[\text{Fe}^{\text{II}}(\text{phen})_2(\text{CN})_2]} &= k'_{\text{obs}} dt, \end{aligned} \quad (15)$$

$$\begin{aligned} \int_{[\text{Fe}^{\text{II}}(\text{phen})_2(\text{CN})_2]_0}^{[\text{Fe}^{\text{II}}(\text{phen})_2(\text{CN})_2]_t} \frac{d[\text{Fe}^{\text{II}}(\text{phen})_2(\text{CN})_2]}{[\text{Fe}^{\text{II}}(\text{phen})_2(\text{CN})_2]} &= k'_{\text{obs}} \int_0^t dt \\ \ln [\text{Fe}^{\text{II}}(\text{phen})_2(\text{CN})_2]_t - \ln [\text{Fe}^{\text{II}}(\text{phen})_2(\text{CN})_2]_0 &= k'_{\text{obs}} t \end{aligned} \quad (16)$$

As we know that in the second phase of the reaction, we have an initial concentration of the product in the reaction mixture at zero time point in this phase. Hence,

$$\begin{aligned} \ln [\text{Fe}^{\text{II}}(\text{phen})_2(\text{CN})_2]_0 &\neq 0 \\ \ln \frac{[\text{Fe}^{\text{II}}(\text{phen})_2(\text{CN})_2]_t}{[\text{Fe}^{\text{II}}(\text{phen})_2(\text{CN})_2]_0} &= k'_{\text{obs}} t, \end{aligned} \quad (17)$$

$$\ln [\text{Fe}^{\text{II}}(\text{phen})_2(\text{CN})_2]_t = \ln [\text{Fe}^{\text{II}}(\text{phen})_2(\text{CN})_2]_0 + k'_{\text{obs}} t, \quad (18)$$

where

$$k'_{\text{obs}} = k_2 [\text{FcCOMe}/\text{FcCHOHMe}] \quad (13)$$

This is important to specify here that according to Eq. (17), under pseudo-first order condition, the value of the observed pseudo-first order rate constant should not change with increasing or decreasing the concentration of the reactant, Fe^{III} complex, that was not in excess. Considering and implementing Beer-Lambert law on Eq. (18), we get Eq. (19):

$$\begin{aligned} \ln \frac{[\text{absorbance}]_t}{\varepsilon b} &= \ln \frac{[\text{absorbance}]_0}{\varepsilon b} + k'_{\text{obs}} t \\ \ln [\text{absorbance}]_t - \ln \varepsilon b &= (\ln [\text{absorbance}]_0 - \ln \varepsilon b) + k'_{\text{obs}} t \\ \ln [\text{absorbance}]_t - \ln \varepsilon b &= \ln [\text{absorbance}]_0 - \ln \varepsilon b + k'_{\text{obs}} t \\ \ln [\text{absorbance}]_t &= \ln [\text{absorbance}]_0 + k'_{\text{obs}} t \end{aligned} \quad (19)$$

According to Eq. (19), if a graph is drawn between \ln absorbance at time point ‘ t ’ versus time, this should be a straight line with an intercept (\ln absorbance at zero time point) and a slope (pseudo-first order rate constant, k'_{obs}). We obtained the values of k'_{obs} from our data by implementing Eq. (19).

Results and discussion

Kinetic parameters

In order to study the kinetics of the reaction(s), we determined the effects of reactants and different parameters on the rate constants in each phase. The plots (Figures S3–S4, supplementary data) of absorbance versus time, according to Eqs. (11) and (19) provided the values of the zeroth order kinetic data (ϵk_{obs}) and the observed pseudo-first order rate constant (k'_{obs}). The linear plots for each experiment show an initial zeroth order and next a first order with respect to $[\text{Fe}^{\text{III}}(\text{phen})_2(\text{CN})_2]^+$ in the first phase and second phase of the reaction(s), respectively. The values of ϵk_{obs} and k'_{obs} did not change by varying the concentration of $[\text{Fe}^{\text{III}}(\text{phen})_2(\text{CN})_2]^+$ in the reaction mixture keeping all other parameters constant (Fig. 1). This behavior justified appropriateness of the composition(s) of the reaction mixture(s) for pseudo-first order condition.

We did not observe any change in the value of ‘ ϵk_{obs} ’, when the concentration of FcCOME or FcCHOHMe was increased in the reaction mixture at constant $[\text{Fe}^{\text{III}}(\text{phen})_2(\text{CN})_2]^+$ and other parameters. However, the value of k'_{obs} increased in each case, FcCOME or FcCHOHMe. The rising nature of the values of k'_{obs} was different with respect to FcCOME or FcCHOHMe. In case

of FcCHOHMe, a linear plot was observed with an intercept and a positive slope (Fig. 2). The results are in accordance with Eqs. (8) and (13). According to Eqs. (8) and (13), we must obtain an intercept equivalent to k_1 or zero order rate constant and a slope equivalent to k_2 or an overall second order rate constant (first order with respect to each of $[\text{Fe}^{\text{III}}(\text{phen})_2(\text{CN})_2]^+$ and FcCHOHMe), respectively. Our data and results highlight a zeroth order in the first phase of the reaction and a first order in the second phase of the reaction with respect to FcCHOHMe. We observed an ascending curvature when k'_{obs} was plotted against the concentration of FcCOME (Fig. 2) with an intercept. The intercept provides the value of the zero order rate constant (k_1) for the reaction between $[\text{Fe}^{\text{III}}(\text{phen})_2(\text{CN})_2]^+$ and FcCOME, and confirms the first phase of the reaction. The ascending curvature indicated that although the value of k'_{obs} increases with increasing concentration of FcCOME, there is a certain reactant in the reaction mixture that acts as the limiting reactant. The curvature became bent at the higher concentrations of FcCOME and the increase in the value of k'_{obs} was comparatively slower than that at the lower concentrations. This may be because of the protonation of the carbonyl group in the organometallic compound, FcCOME.

Protonation is the well-known character of the carbonyl group, and in 80% aqueous dioxane there must be a limited concentration of the protons in the reaction medium. The phenomenon of autoionization and autoionization constants of different solvents and their mixtures are mentioned in detail in Khattak (2011). At the higher concentrations of the compound, the carbonyl group is frequently available for the protonation, but under the limited concentration of protons the expected concentration of protonated or conjugate acid of acetylferrocene remains limited because of the equilibrium between protonated and non-protonated FcCOME. In

Fig. 1 Kinetic data with respect to $[\text{Fe}^{\text{III}}(\text{phen})_2(\text{CN})_2]^+$ in 80% aqueous dioxane. The experimental conditions were maintained at 0.18 mM (ionic strength, I), 304 ± 0.5 K (for FcCOME) and 291 ± 0.5 K (for FcCHOHMe). The circle and triangle represent the effect of variation in the concentration of $[\text{Fe}^{\text{III}}(\text{phen})_2(\text{CN})_2]^+$ on ϵk_{obs} (triangle), and k'_{obs} (circle) at 1.3 mM [FcCOME]. The square and dash show the impact on ϵk_{obs} ; square, k'_{obs} ; dash, at 1.3 mM [FcCHOHMe]

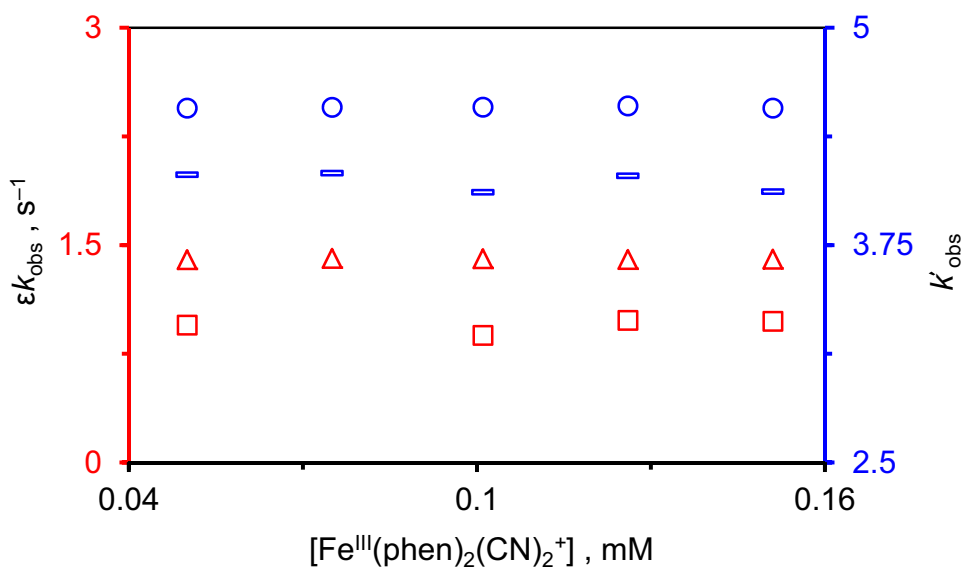


Fig. 2 Effect of [FcCOMe] and [FcCHOHMe] on (ϵk_{obs} ; triangle, k'_{obs} ; circle) and (ϵk_{obs} ; square, k'_{obs} ; dash), respectively, in 80% aqueous dioxane. The experimental parameters were 0.08 mM $[\text{Fe}^{\text{III}}(\text{phen})_2(\text{CN})_2]^+$, 0.18 mM (I), 304 ± 0.5 K (for FcCOMe) and 291 ± 0.5 K (for FcCHOHMe). The circle and dash mention k'_{obs} at 1:1 concentration ratio between oxidizing and reducing agents

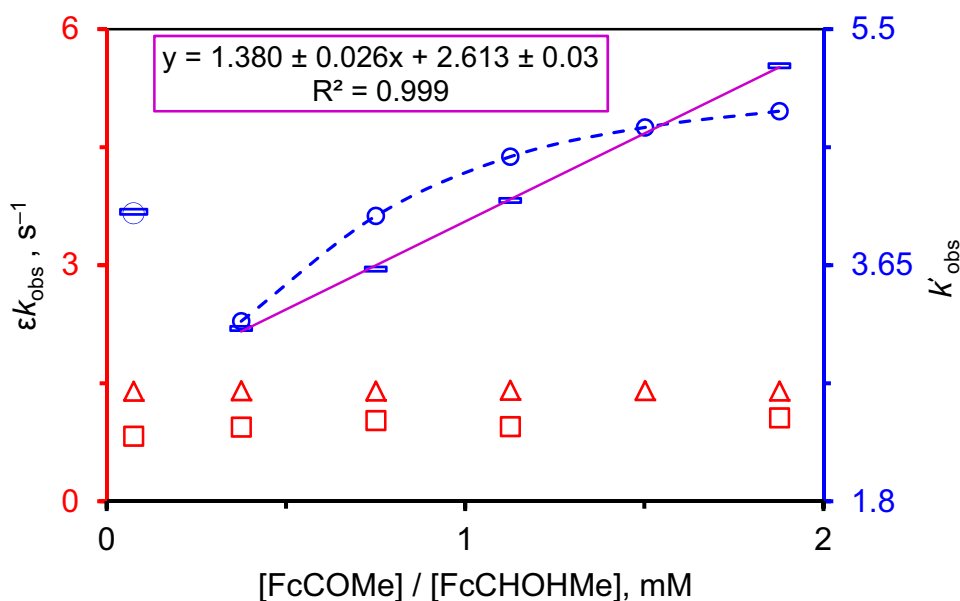
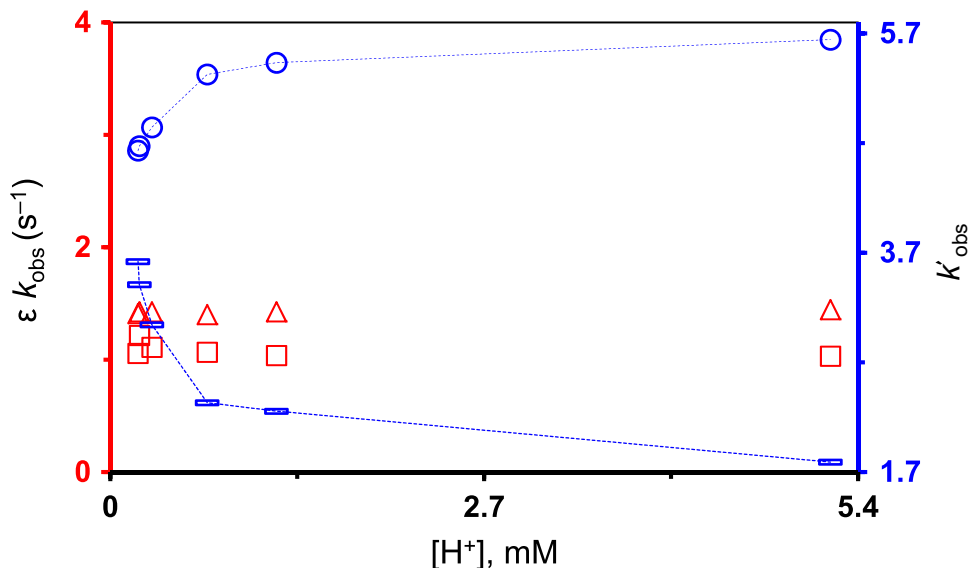


Fig. 3 Effect of protons on the rate constants (ϵk_{obs} ; triangle, k'_{obs} ; circle) of FcCOMe, and (ϵk_{obs} ; square, k'_{obs} ; dash) of FcCHOHMe. The experimental conditions were maintained at 5.1 mM (I), 0.08 mM $[\text{Fe}^{\text{III}}(\text{phen})_2(\text{CN})_2]^+$ and 0.75 mM $[\text{FcCOMe}]$ or $[\text{FcCHOHMe}]$



order to justify our observations and results, we studied the effect of variation in the concentration of protons on the rate constants, ' ϵk_{obs} ' and ' k'_{obs} ' of each reaction. We maintained the experimental conditions at the concentration ratio of $[\text{Fe}^{\text{III}}(\text{phen})_2(\text{CN})_2]^+ \ll \text{FcCOMe}$ or $\text{FcCHOHMe} \ll [\text{H}^+]$ via adding aqueous HNO_3 and keeping all other parameters constant. In case of the reduction of $[\text{Fe}^{\text{III}}(\text{phen})_2(\text{CN})_2]^+$ by FcCOMe the value of k'_{obs} enhanced by enriching the reaction mixture with protons, and decreased on the other way in the case of the reaction of FcCHOHMe. The zeroth order rate constant remained unaffected in each case, which justified an initial zeroth order with respect to the oxidizing and the reducing agents in the first phase of the reactions. The results are illustrated in Fig. 3. The variation of k'_{obs}

with respect to the concentration of protons in the reaction mixture is the confirmation of participation of the protonated acetylferrocene and α -methylferrocenemethanol in the mechanisms of electron transfer. The bending curvatures, which become almost constant and do not show further increase or decrease at the higher concentration of protons demonstrate FcCOMe or FcCHOHMe as the limiting reactants in the reaction mixture. The increasing value of k'_{obs} in case of FcCOMe confirms the formation of protonated acetylferrocene or conjugate acid of acetylferrocene, FcC^+OHMe , and its participation to reduce $[\text{Fe}^{\text{III}}(\text{phen})_2(\text{CN})_2]^+$ through first order kinetics in the second phase of the reaction. Meanwhile, the decrease in the value of k'_{obs} helps to identify the formation of protonated

methylferrocenemethanol, $\text{FcCHO}^+\text{H}_2\text{Me}$, and its oxidation during the reaction. Our observations and results showed the key role of protonation of the reacting entities in the electron transfer processes, and also the probabilities of the changes of the mechanistic pathways by involvement of the protonated species. This facet is prominent in acetylferrocene (FcCOMe) and α -methylferrocenemethanol (FcCHOHMe), and plays a leading role in the redox reactions of these organometallic compounds. We probed our target reactions in aqueous dioxane. This co-solvent system facilitates hydrogen bonding and produces acidic character in the medium. This decreases the pH and provides a base for the protonation of FcCOMe and FcCHOHMe at oxygen atom. The protons bind to the electron-rich oxygen atoms, and produce monoprotonated compounds such as FcCO^+HMe and $\text{FcCHO}^+\text{H}_2\text{Me}$. The protonated acetylferrocene is stabilized by resonance, and yields an unsaturated compound with a carbonium atom, FcC^+OHMe . We further refined our results to differentiate and identify those species among protonated and non-protonated, which take part in the rate-determining step of each reaction. This refinement of the results was carried out by studying the effects of ionic strength and dielectric constant on the observed rate constants (ϵk_{obs} and k'_{obs}) considering the transition state theory of reactions in solution.

Effect of ionic strength and dielectric constant

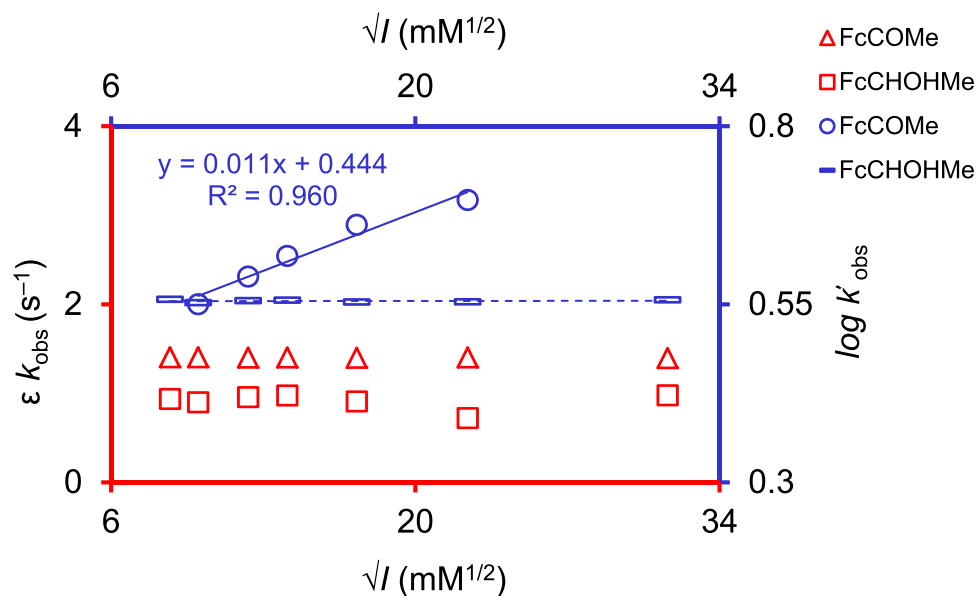
The effect of ionic strength (I) on the rate constants in the first and second phase of the reactions was studied by varying ionic strength of the medium (80% aqueous dioxane) through potassium nitrate (KNO_3) at $[\text{Fe}^{\text{III}}(\text{phen})_2(\text{CN})_2^+] \ll [\text{FcCOMe}]$ or $[\text{FcCHOHMe}]$, keeping

other parameters constant. The value of the rate constants ' ϵk_{obs} ' remained unchanged upon increasing the ionic strength for each reaction. During the reaction of FcCOMe , the value of k'_{obs} increased with increasing ionic strength and it was unaffected during the reaction of FcCHOHMe . The data were analyzed by implementing following equation of transition state theory:

$$\log k'_{\text{obs}} = \log k_{\text{obs}}^{\text{ideal}} + 2Az_A z_B \sqrt{I} \quad (20)$$

Different terms in Eq. (20) carry different meanings. For example, $\log k'_{\text{obs}}$ is the base 10 log of the observed pseudo-first order rate constant; A is the Debye–Hückel constant and it depends upon the dielectric constant of the medium and temperature; $z_A z_B$ is the product of the charges, which takes part in the rate-determining step, and, $\log k_{\text{obs}}^{\text{ideal}}$ is the base 10 log of the observed pseudo-first order rate constant at zero ionic strength or ideal condition. The results are shown in Fig. 4. When we drew ϵk_{obs} versus \sqrt{I} , we did not observe any impact of ionic strength on the rate constant in the first phase of each reaction, which confirmed zeroth order kinetics with respect to the oxidizing and reducing agent in this phase of the reactions. The plot of $\log k'_{\text{obs}}$ against \sqrt{I} is a straight line with a zero slope in case of FcCHOHMe , and, it is a straight line with a positive value of the slope in case of FcCOMe . These patterns of the graphs in the second phase of the reactions are very helpful to differentiate among the species, protonated and non-protonated $\text{FcCOMe}/\text{FcCHOHMe}$, which are taking part in the fast-step and the rate-determining or slow-step. The positive value of the slope indicates participation of protonated acetylferrocene (FcCO^+HMe) in the slow- or rate-determining step of the reaction because the charge product of the reacting entities

Fig. 4 Effect of ionic strength on the rate constants (ϵk_{obs} ; triangle, k'_{obs} ; circle) of FcCOMe , and (ϵk_{obs} ; square, k'_{obs} ; dash) of FcCHOHMe in 80% aqueous dioxane. The experimental conditions were maintained at 0.08 mM ($[\text{Fe}^{\text{III}}(\text{phen})_2(\text{CN})_2^+]$) and 0.75 mM ($[\text{FcCOMe}]$ or $[\text{FcCHOHMe}]$)



in the rate-determining step yields positive value, + 1 from $[\text{Fe}^{\text{III}}(\text{phen})_2(\text{CN})_2]^+$ and + 1 from FcCO^+HMe . However, non-protonated acetylferrocene (FcCOMe) is oxidized in the fast-step of the reaction between $[\text{Fe}^{\text{III}}(\text{phen})_2(\text{CN})_2]^+$ and FcCOMe . The neutral effect of ionic strength upon k'_{obs} identified and justified participation of non-protonated FcCHOHMe in the slow- or rate-determining step because the charge product + 1 from $[\text{Fe}^{\text{III}}(\text{phen})_2(\text{CN})_2]^+$ and 0 from FcCHOHMe gives an overall zero term in Eq. (20), whilst that of protonated $\text{FcCHO}^+\text{H}_2\text{Me}$ in the fast-step of the reaction between $[\text{Fe}^{\text{III}}(\text{phen})_2(\text{CN})_2]^+$ and FcCHOHMe .

The effect of dielectric constant according to the following formulation (21) of the transition state theory confirmed our results, which we obtained on the basis of ionic strength.

$$\log k_{\text{obs}}^{\text{ideal}} = \ln k_0 + \frac{z_A z_B e^2}{4\pi\epsilon_0\epsilon_r r_{\#} kT} \quad (21)$$

In Eq. (21), $\ln k_{\text{obs}}^{\text{ideal}}$ and $\ln k_0$ refer to the natural logarithm of the observed pseudo-first order rate constant at zero ionic strength and the natural logarithm of the observed pseudo-first order rate constant at infinite dielectric constant, respectively. $z_A z_B$ is the product of the charges participating in the rate-determining step; e is the electron charge; ϵ_0 is the vacuum permittivity; ϵ_r is the dielectric constant of the medium; $r_{\#}$ is the distance between the charges in the activated complex; k is Boltzmann constant and T is Kelvin temperature.

We decreased the dielectric constant of the medium by increasing % volume of dioxane in water from 90% to 50% aqueous dioxane. We determined the values of ' ϵk_{obs} ' and ' k'_{obs} ' under ideal condition or the condition when the ionic strength was zero for each reaction with the help of Eq. (20). The values ' ϵk_{obs} ' and ' k'_{obs} ' were drawn against

the reciprocal of the dielectric constant of the medium according to Eq. (21) for the data obtained for each reaction. The results are displayed in Fig. 5. The value of ϵk_{obs} did not change with a decreasing dielectric constant as was supposed due to the zeroth order kinetics in the first phase of each reaction. We obtained a straight line with a negative slope when we plotted the natural logarithm of the observed pseudo-first order rate constant at zero ionic strength against the reciprocal of the dielectric constant for the reaction of FcCOMe . The negative slope confirms oxidation of the monopositive FcCO^+HMe by monopositive $[\text{Fe}^{\text{III}}(\text{phen})_2(\text{CN})_2]^+$ in the rate-determining step. This further explained the oxidation of neutral FcCOMe by $[\text{Fe}^{\text{III}}(\text{phen})_2(\text{CN})_2]^+$ during the fast-step. We observed a straight line with a zero slope, in other words, no effect, while we drew a graph between the natural logarithm of the observed pseudo-first order rate constant at zero ionic strength and the reciprocal of the dielectric constant for the reaction between FcCHOHMe and $[\text{Fe}^{\text{III}}(\text{phen})_2(\text{CN})_2]^+$. A zero slope means one of the reacting entities carries a zero charge, and that is why the multiplication product of the last term in Eq. (21) appears to be zero. These results affirmed oxidation of the neutral FcCHOHMe by $[\text{Fe}^{\text{III}}(\text{phen})_2(\text{CN})_2]^+$ in the slow-step and the monopositive $\text{FcCHO}^+\text{H}_2\text{Me}$ by $[\text{Fe}^{\text{III}}(\text{phen})_2(\text{CN})_2]^+$ in the fast-step (zero order phase).

Thermodynamic parameters of activation

The reactions were probed at different temperatures to evaluate the thermodynamic parameters of activation. The temperature change did not affect the values of ϵk_{obs} of the two reactions (Fig. 6a). The figure of k'_{obs} increased in both cases. The activation energy ' E_A ' and ' A ' factor of the redox reactions were estimated from the values of the slope

Fig. 5 Effect of dielectric constant on the rate constants (ϵk_{obs} ; triangle, k'_{obs} ; circle) of FcCOMe , and (ϵk_{obs} ; square, k'_{obs} ; dash) of FcCHOHMe . The experimental conditions were maintained at 0.08 mM ($[\text{Fe}^{\text{III}}(\text{phen})_2(\text{CN})_2]^+$) and 0.75 mM ($[\text{FcCOMe}]$ or $[\text{FcCHOHMe}]$)

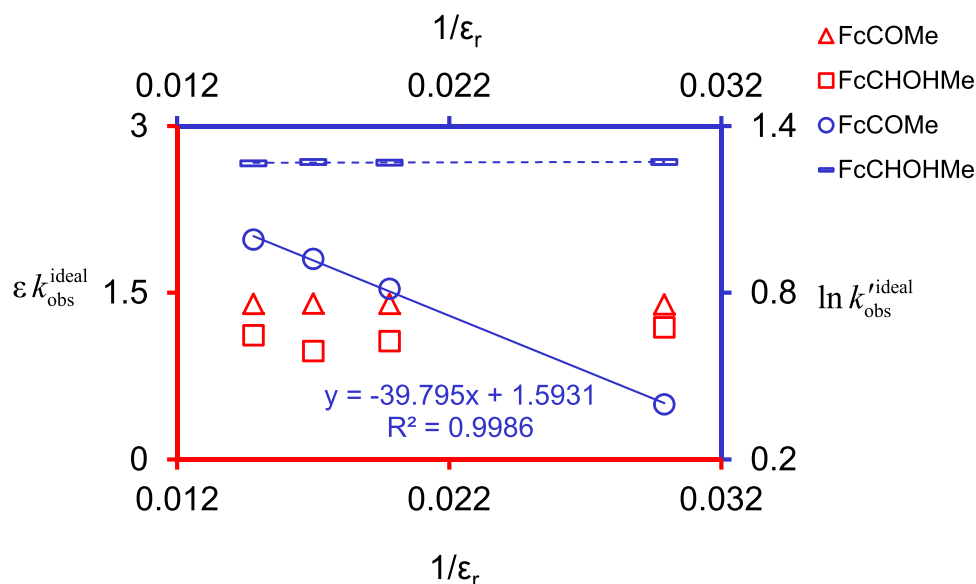
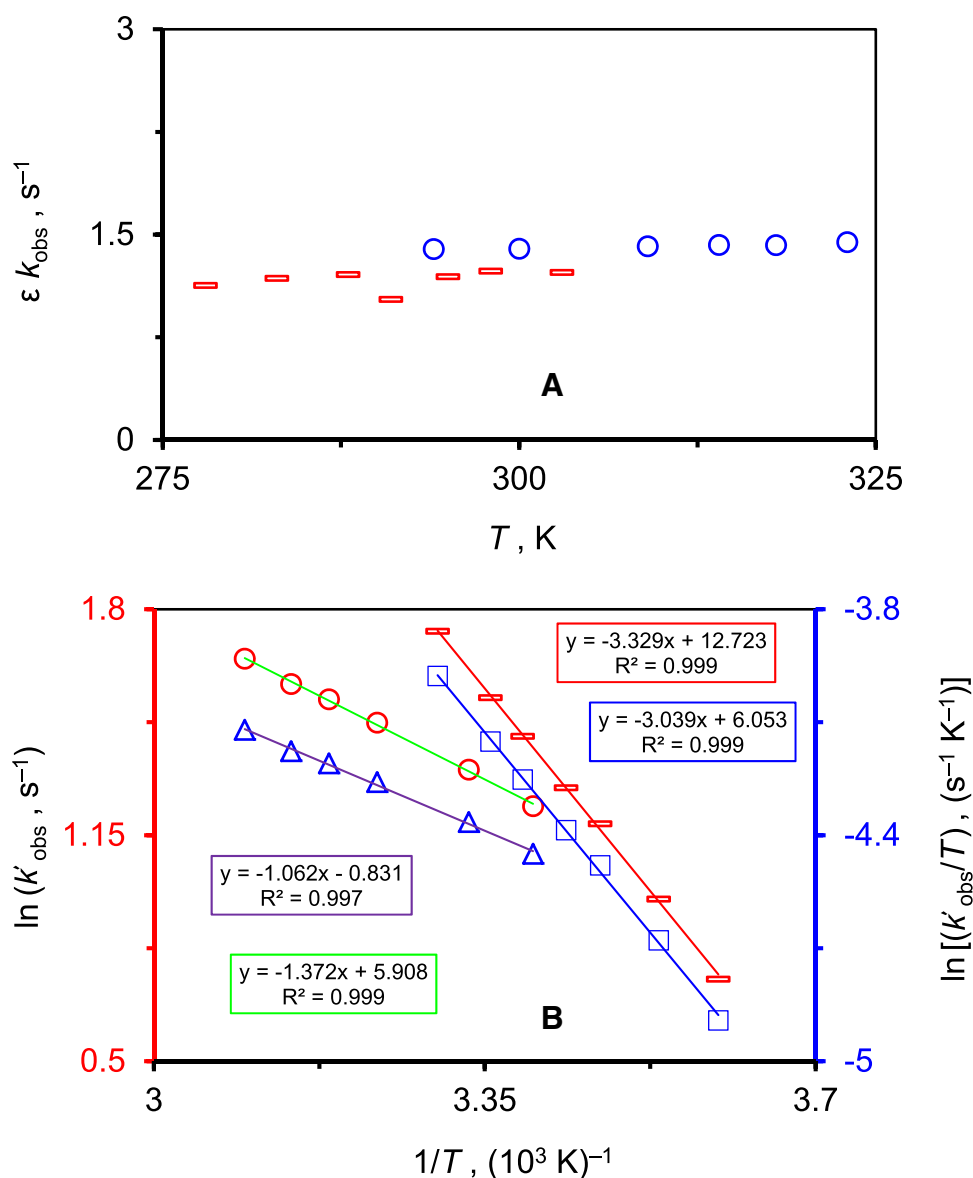


Fig. 6 Plot **a** represents the effect of temperature on ϵk_{obs} ; dash, of FcCOMe, and ϵk_{obs} ; circle, of FcCHOHMe. Plot **b** shows the fitting of Arrhenius and Eyring equations, where triangle and circle correspond to FcCOMe, and, square and dash to FcCHOHMe. The experimental conditions were maintained at 0.08 mM ($[\text{Fe}^{\text{III}}(\text{phen})_2(\text{CN})_2^+]$) and 0.75 mM ($[\text{FcCOMe}]$ or $[\text{FcCHOHMe}]$)



and intercept, respectively, by drawing a graph of, $\ln k'_{\text{obs}}$ versus $1/T$, according to the Arrhenius equation (Fig. 6b). The values of the thermodynamic parameters of activation, such as enthalpy and entropy of activation (ΔH^\ddagger , ΔS^\ddagger) were determined by plotting, $\ln (k'_{\text{obs}}/T)$ against $1/T$, according to the Eyring equation (Fig. 6b). The Gibbs energy of activation (ΔG^\ddagger) was then calculated by employing equation, $\Delta G^\ddagger = \Delta H^\ddagger - T\Delta S^\ddagger$. These estimated figures of E_A , A , ΔH^\ddagger , ΔS^\ddagger and ΔG^\ddagger are displayed in Table 1.

The redox reaction between $[\text{Fe}^{\text{III}}(\text{phen})_2(\text{CN})_2]^+$ and FcCOMe, and or, FcCHOHMe has been classified as endothermic. The value of the enthalpy of activation (ΔH^\ddagger) and Gibbs free energy of activation (ΔG^\ddagger) have numerals with a + sign. The rate(s) of reaction(s) increased upon increasing the temperature in the phase where it follows an overall second order kinetics.

Table 1 Thermodynamic parameters of activation

	FcCOMe	FcCHOHMe
E_A (kJ mol ⁻¹)	11.41	27.7
A (s ⁻¹)	369	337,055
ΔH^\ddagger (kJ mol ⁻¹)	8.83	25.3
ΔS^\ddagger (J mol ⁻¹ K ⁻¹)	-204.45	-147
ΔG^\ddagger (kJ mol ⁻¹)	70.6 at 302 K	69.7 at 302 K

The electrostatic terms, in the equation of the rate constant based upon the transition state theory, predict the nature of the involved charges and the solvent interaction with the species participating in the reaction while forming the activated complex. A smaller value of ΔH^\ddagger with a loss of entropy ΔS^\ddagger (larger -ve numeral) suggests that the

reacting entities carry like charges, which demonstrates a characteristic associative mechanism. However, a reverse case, the +ve contribution to ΔH^\ddagger with a gain in entropy ΔS^\ddagger (smaller –ve numeral) is observed for unlike charges with an associative mechanism.

A close examination of the thermodynamic parameters of activation (Table 1) helps to demonstrate small E_A , ΔH^\ddagger and –ve ΔS^\ddagger value(s) to be a characteristic representative of an associative mechanism in case of acetylferrocene. The reaction was hardly dependent upon temperature. This provides a strong support to the electron-donating facet of $[\text{FcC}^+\text{OHMe}]$ in the rate-determining or slow-step. It has already been discussed that the unsaturated protonated acetylferrocene is highly energetic and reactive. It means that the monopositive species needs small quanta of energy to cross the barrier of activation energy to yield products. We observed this in our study. A low value of the enthalpy of activation reinforces our findings. Contrary to that, we observed the normal and reasonable values of E_A , ΔH^\ddagger and –ve ΔS^\ddagger during the oxidation of α -methylferrocenemethanol because of the participation of saturated and stable species $[\text{FcCHOHMe}]$ in the rate-determining step.

Conclusions

The results obtained from the kinetic data and its thermodynamic aspect refer to the existence of equilibrium between protonated and unprotonated acetylferrocene, and also α -methylferrocenemethanol. The unprotonated and protonated species of these compounds take part in the electron transfer process, and donate electron to $[\text{Fe}^{\text{III}}(\text{phen})_2(\text{CN})_2]^+$. Protonation of FcCOMe generates conjugate acid, FcC^+OHMe , in acidic medium (Arnett and Bushick 1962; Rubalcava and Thomson 1963). Our investigation highlights the vital role of OH group of either FcC^+OHMe or FcCHOHMe in the oxidation of FcCOMe and FcCHOHMe . This study evinces that the rate of reaction of the subject compounds is controlled by OH (hydroxyl)-containing compounds such as saturated α -methylferrocenemethanol or unsaturated conjugate acid of acetylferrocene. This brings us to the conclusion that the protonation of these compounds changes their reactivity in chemical and biochemical processes either partially or completely, leading to significant changes in the mechanism.

Acknowledgements The authors are indebted to the HEJ Research Institute of Chemistry, University of Karachi, Pakistan, for providing analytical services to carry out IR and microanalytical characterization of the synthesized compound(s).

References

- Arnett EM, Bushick RD (1962) Quantitative estimates of the strong electron donor properties of metallocenyl nuclei. *J Org Chem* 27(1):111–115. <https://doi.org/10.1021/jo01048a028>
- Baciocchi E, Floris B, Muraglia E (1993) Reactions of ferrocene and acetylferrocene with carbon-centered free radicals. *J Org Chem* 58(8):2013–2016. <https://doi.org/10.1021/jo00060a011>
- Blake R, White KJ, Shute EA (1991) Mixed ligand complexes of iron with cyanide and phenanthroline as new probes of metalloprotein electron transfer reactivity. Analysis of reactions involving rusticyanin from *Thiobacillus ferrooxidans*. *J Biol Chem* 266(29):19203–19211. <http://www.jbc.org/content/266/29/19203.full.pdf>
- Casas JS, Castaño MV, Cifuentes MC, García-Monteagudo JC, Sánchez A, Sordo J, Touceda A (2007) Interaction of organolead(IV) derivatives with formyl- and acetylferrocene thiosemicarbazones: coordination versus dephenylation or reductive elimination processes. *J Organometal Chem* 692(11):2234–2244. <https://doi.org/10.1016/j.jorganchem.2007.01.049>
- Connelly NG, Geiger WE (1996) Chemical redox agents for organometallic chemistry. *Chem Rev* 96(2):877–910. <https://doi.org/10.1021/cr940053x>
- Floris B (2015) Ferrocene in agriculture: from agrochemicals and soil remediation to selective chemosensors. *Chem Biol Technol Agric* 2(1):15. <https://doi.org/10.1186/s40538-015-0038-0>
- Gao Z-N, Ma J-F, Liu W-Y (2005a) Electrocatalytic oxidation of sulfite by acetylferrocene at glassy carbon electrode. *Appl Organometal Chem* 19(11):1149–1154. <https://doi.org/10.1002/aoc.975>
- Gao Z-N, Zhang J, Liu W-Y (2005) Electrocatalytic oxidation of *n*-acetyl-L-cysteine by acetylferrocene at glassy carbon electrode. *J Electroanal Chem* 580(1):9–16. <http://www.sciencedirect.com/science/article/B6TGB-4FXV79B-6/2/31261f9ef9b2fb7ce46753fbff8415>
- Jong S-J, Fang J-M, Lin C-H (1999) The reactions of acylferrocenes with samarium diiodide: reduction, deoxygenation, reductive coupling and rearrangement. *J Organometal Chem* 590(1):42–45. [https://doi.org/10.1016/S0022-328X\(99\)00411-8](https://doi.org/10.1016/S0022-328X(99)00411-8)
- Khattak R (2011) Comparative kinetic study for the electron transfer reactions of some iron complexes. In: Department of Chemistry, University of Karachi, Karachi, p 501
- Khattak R, Naqvi II, Farrukh MA (2008) Kinetics and mechanism of the oxidation of a ferrous complex with an α , α' -diimine chelate ligand by ceric sulfate in aqueous acidic medium by UV-Vis absorption spectroscopy. *J Iran Chem Soc* 5(4):631–640. <https://doi.org/10.1007/BF03246144>
- Khattak R, Naqvi II, Summer S, Sayed M (2016) Mechanism of the oxidation of 1-(ferrocenyl)-ethanone/ethanol by dicyanobis(phenanthroline)iron(III). *Arab J Chem*. <https://doi.org/10.1016/j.arabjc.2016.05.007>
- Matsumoto M, Tarumi T, Sugimoto K-I, Kagayama N, Funahashi S, Takagi HD (1997) Oxidation reaction of L-ascorbic acid by dicyanobis(1,10-phenanthroline)iron(III) in dimethyl sulfoxide at elevated pressure: evidence for adiabatic electron transfer. *Inorg Chim Acta* 255:81–85. [https://doi.org/10.1016/S0020-1693\(96\)05342-X](https://doi.org/10.1016/S0020-1693(96)05342-X)
- Osella D, Ferrali M, Zanello P, Laschi F, Fontani M, Nervi C, Caviglioglio G (2000) On the mechanism of the antitumour activity of ferrocenium derivatives. *Inorg Chim Acta* 306:42–48. [https://doi.org/10.1016/S0020-1693\(00\)00147-X](https://doi.org/10.1016/S0020-1693(00)00147-X)
- Patra M, Gasser G (2017) The medicinal chemistry of ferrocene and its derivatives. *Nat Rev Chem* 1:0066. <https://doi.org/10.1038/s41570-017-0066>

- Pelizzetti E, Mentasti E, Pramauro E (1978) Outer-sphere oxidation of ascorbic acid. *Inorg Chem* 17(5):1181–1186. <https://doi.org/10.1021/ic50183a018>
- Pladziewicz JR, Espenson JH (1973) Kinetics and mechanisms of some electron transfer reactions of ferrocenes. *J Am Chem Soc* 95(1):56–63. <https://doi.org/10.1021/ja00782a011>
- Quirk PF, Kratochvil B (1970) Determination of ferrocene derivatives by oxidation with copper(ii) in acetonitrile. *Anal Chem* 42(4):535–536. <https://doi.org/10.1021/ac60286a035>
- Realista S, Quintal S, Martinho PN, Melato AI, Gil A, Esteves T, Carvalho MD, Ferreira LP, Vaz PD, Calhorda MJ (2017) Electrochemical studies and potential anticancer activity in ferrocene derivatives. *J Coord Chem* 70(2):314–327. <https://doi.org/10.1080/00958972.2016.1257125>
- Rubalcava HE, Thomson JB (1963) A spectroscopic study of the protonation of acetylferrocenes. Hydrogen-deuterium exchange in the conjugate acids. *J Phys Chem* 67(2):310–313. <https://doi.org/10.1021/j100796a023>
- Saleem M, Yu H, Wang L, Zain ul A, Khalid H, Akram M, Abbasi NM, Huang J (2015) Review on synthesis of ferrocene-based redox polymers and derivatives and their application in glucose sensing. *Analyt Chim Acta* 876(Supplement C):9–25. <https://doi.org/10.1016/j.aca.2015.01.012>
- Sasaki Y, Pittman CU (1973) Acid-catalyzed reaction of acetylferrocene with triethyl orthoformate. *J Org Chem* 38(21):3723–3726. <https://doi.org/10.1021/jo00961a014>
- Schilt AA (1960) Mixed ligand complexes of iron(ii) and (iii) with cyanide and aromatic di-imines. *J Am Chem Soc* 82(12):3000–3005. <https://doi.org/10.1021/ja01497a007>
- Shago RF, Swarts JC, Kreft E, Rensburg CEJV (2007) Antineoplastic activity of a series of ferrocene-containing alcohols. *Anticancer Res* 27:3431–3434. <http://citeseerx.ist.psu.edu/viewdoc/download?doi=10.1.1.1022.7131&rep=rep1&type=pdf>
- Summer S, Naqvi II, Khattak R, Gulzar S, Reyaz F (2016) Kinetics and mechanism of $[\text{Fe}(\text{bipy})_3]^{2+}$ and $[\text{BrO}_3^-]$ system in aqueous acidic medium. *J Chem Soc Pak* 38(03):384–389. <http://www.jcsp.org.pk/ViewByVolume.aspx?v=1209&i=VOLUME%2038,%20NO3,%20JUNE-2016>
- Takagi HD, Kagayama N, Matsumoto M, Tarumi T, Funahashi S (1995) Mechanistic study of oxidation reactions of hydroquinone, catechol and l-ascorbic acid by dicyanobis(1,10-phenanthroline) iron(iii) in dimethyl sulfoxide. *J Mol Liq* 65–66:277–280. [https://doi.org/10.1016/0167-7322\(95\)00827-0](https://doi.org/10.1016/0167-7322(95)00827-0)
- Xu X, Nolan SP, Cole RB (1994) Electrochemical oxidation and nucleophilic addition reactions of metallocenes in electrospray mass spectrometry. *Anal Chem* 66(1):119–125. <https://doi.org/10.1021/ac00073a021>